Positive Feedback by a Potassium-Selective Inward Rectifier Enhances Tuning in Vertebrate Hair Cells

M. B. Goodman* and J. J. Art#
*Committee on Neurobiology, The University of Chicago, Chicago, Illinois 60637, and #Department of Anatomy and Cell Biology, University of Illinois College of Medicine, Chicago, Illinois 60612 USA

ABSTRACT Electrical resonance in vertebrate hair cells shapes receptor potentials and tunes each cell to a narrow band of frequencies. We have investigated the contribution of a potassium-selective inward rectifier (IR) to electrical resonance, isolating outward current carried by IR from other ionic currents active in the physiological voltage range (−75 to −30 mV) using a combination of potassium and calcium channel antagonists. IR expression is tightly regulated in the turtle's auditory epithelium, as revealed by the observation that its size declines systematically with resonant frequency. A critical feature of IR is the rapid inhibition produced by depolarization, which results in a negative slope in the steady-state current-voltage relation in the vicinity of the resting potential (−50 mV). The increasing block of outward current produced by depolarization is functionally equivalent to activating an inward current, suggesting that IR provides positive feedback and, in hair cells, serves an electrical function ordinarily reserved for voltage-dependent sodium and calcium currents. Additional support for this idea comes from the observation that superfusion with cesium selectively reduces IR and eliminates resonance in cells tuned to low frequencies and degrades resonant quality in cells tuned to more than 50 Hz.

INTRODUCTION

Potassium-selective inward rectifiers (IRs) are widely distributed among tissues and represent one of several ionic channels that shape cellular behavior. Recently our understanding of the molecular basis of inward rectification has expanded through studies of cloned channel proteins. These studies have focused on the mechanism of inward rectification, including the role of voltage-dependent block by intracellular divalent cations (Nichols et al., 1994; Stanfield et al., 1994a) and polyamines (Ficker et al., 1994; Lopatin et al., 1994; Fakler et al., 1995). However, the functional significance of IR can only be understood when its behavior is examined in its native environment. Because hair cells contain relatively few, well-characterized ionic channels that can be eliminated pharmacologically, they are a particularly attractive venue in which to study IR function. An additional advantage offered by the hair cell is the primacy of electrical resonance and our understanding of the role ionic currents play in shaping the receptor potentials that give rise to auditory sensation (Crawford and Fettiplace, 1980; Lewis and Hudspeth, 1983; Art and Fettiplace, 1987).

Perhaps the most frequently cited role for IR relates to its ability to maintain the cell's resting membrane voltage near the K^+ equilibrium potential, E_K (see Hille, 1992). Inward rectifiers are unlikely to play a similar role in turtle hair cells, because the average zero-current potential (−50 mV) is 40 mV positive to E_K (Crawford and Fettiplace, 1980). The importance of IR for normal hair cell function was suggested to us by the tight regulation of channel expression revealed by the observation that IR is larger in cells tuned to the lowest frequencies and declines systematically with increasing resonant frequency (Goodman and Art, 1993). Previously, other currents whose magnitude vary with frequency, such as calcium or calcium-activated potassium currents, have been demonstrated to be important in determining the quality and frequency of hair cell resonance (Art et al., 1993). The systematic decrease in IR with resonant frequency may also be a general property of hearing organs, because a qualitatively similar distribution of IR current (Fuchs and Evans, 1990) and cIRK1 transcripts (Navaratnam et al., 1995) exists in the chick cochlea.

Two types of inwardly rectifying currents have been described in vertebrate hair cells since inward rectification of membrane current was first noted in the frog sacculus (Corey and Hudspeth, 1979). They are IR, an inward rectifier selective for K^+, and I_h, a hyperpolarization-activated current permeable to both Na^+ and K^+ (Holt and Eatock, 1995). Here, we examine the macroscopic behavior of the K^+-selective hair cell IR and its part in electrical resonance, paying particular attention to its voltage and time dependence in the physiological range (−75 to −30 mV). Although the K^+ current is outward in this range, the steady-state *I-V* relation has a negative slope, indicating that IR is inhibited with depolarization and is capable of generating positive feedback. The form of its *I-V* curve can be reproduced by assuming IR has a constant conductance and is subject to voltage-dependent block by an intracellular particle or particles. Its form can also be modulated by variations in external K^+ concentration, raising the possibility that the voltage range in which IR generates positive feedback is a dynamic function of external K^+. We further

Received for publication 8 November 1995 and in final form 3 April 1996.

Address reprint requests to Dr. Jonathan J. Art, Department of Anatomy and Cell Biology, University of Illinois College of Medicine, 808 S. Wood, Chicago, IL 60612. Tel.: 312-996-4956; Fax: 312-413-0354; E-mail: jart@uic.edu.

Dr. Goodman's present address is Institute of Neuroscience, 1254 University of Oregon, Eugene, OR 97403.

0006-3495/96/07/430/13 $2.00

demonstrate that the novel role IR plays in enhancing cellular excitability can be revealed in current clamp by using external Cs^+ to selectively inhibit IR and dampen hair cell resonance. A preliminary report of some of this work has appeared (Goodman and Art, 1993)

MATERIALS AND METHODS

Preparation and recording techniques

Auditory hair cells were isolated from a homolog of the cochlea, the basilar papilla of the red-eared turtle (*Trachemys scripta elegans*, carapace length 10–12 cm), using modifications of a standard procedure (Art and Fettiplace, 1987). Briefly, after decapitation of the turtle, the basilar papilla was dissected out, and the preparation was incubated in a low Ca^{2+} saline (Table 1) supplemented with 30 μg/ml bacterial protease type XXIV (Sigma P8038). After the tectorial membrane was removed, the epithelium was incubated in either a low Ca^{2+} saline containing 0.5 mg/ml papain, 2.5 mM L-cysteine, and 0.1 mg/ml bovine serum albumin, or EDTA-buffered saline ($Ca^{2+} \approx 30$ μM, Mg ≈ 5 mM; see Table 1) containing 200 μg/ml DNase I, type IV. Hair cells were collected while in low Ca^{2+} saline, and plated onto a glass coverslip that was transferred to the stage of an inverted microscope (Zeiss IM) equipped with Nomarski optics. Cells were superfused with either normal saline or saline supplemented with 0.4 mg/ml bovine serum albumin. Experiments were performed at 22–24°C for periods of up to 5 h after decapitation.

Solutions

Cells were exposed to different solutions by means of a six-barreled glass "pan-pipe" (Vitro Dynamics, Rockaway, NJ). Each barrel was of square cross section pulled to an internal diameter of about 75 μm and perfused from a peristaltic pump, a given barrel being selected by means of a remotely controlled miniature solenoid valve (Lee Products, Westbrook, CT). Solution was removed by a U-tube (Krishtal and Pidoplichko, 1980) placed at 90° with respect to the pan-pipe array. This arrangement provided rapid, local solution exchanges.

Extracellular solutions were based on normal turtle saline (Table 1). Drugs applied in excess of 1 mM were substituted for an equimolar concentration of NaCl. Tetraethylammonium (TEA) was obtained as TEA-OH (Aldrich Chemical, Milwaukee, WI) and titrated with HCl to yield a 1 M stock solution. 4-Aminopyridine (4-AP) was diluted from a 30 or 60 mM stock solution prepared daily from solid. After dilution, the pH was adjusted to 7.6 with HCl.

Nisoldipine was prepared as a stock solution in 100% EtOH from powder stored in darkness at −20°C. Solutions containing nisoldipine were protected from exposure to room light because it is readily degraded by illumination (Sanguinetti and Kass, 1984). Calibrated solutions (1 M) of $CaCl_2$ and $MgCl_2$ were purchased from BDH through their U.S. distributor (Gallard-Schlesinger, Carle Place, NY) and Alfa Chemical (Ward Hill, MA), respectively. Unless indicated, all other reagents were obtained from Sigma Chemical (St. Louis, MO). Osmolarity of extracellular (290 mOsm) and intracellular (270 mOsm) solutions was assayed by freezing-point depression (Advanced Instruments, Natick, MA).

Electrophysiology

Hair cell membrane current and voltage were recorded using standard whole-cell patch clamp methods (Hamill et al., 1981). Pipettes were pulled from soda-glass capillaries (S/P Brand, Baxter Scientific) coated with Sylgard 182 and fire-polished immediately before use. Electrodes were filled with a K^+-based solution composed of (in mM): KCl, 125; $CaCl_2$, 0.45; $MgCl_2$, 2.8; K_2EGTA, 5; Na_2ATP, 2.5; KHEPES, 5 (pH 7.2). The measured liquid junction between intracellular solution and normal turtle saline (internal-external solution) was −4.5 mV. Membrane current and voltage were recorded with a modified Yale Mark V amplifier (Art and Fettiplace, 1987). Experiments were recorded with an 8-channel PCM unit (VR-100; Instrutech, Elmont, NY) and analyzed off-line. To avoid jitter, the PCM's clock circuit was used to control digitization. Unless otherwise indicated, the data were filtered at 3.2 kHz (8-pole Bessel filter) and digitized at up to 24 kHz.

All voltages are corrected for liquid junction potentials and errors due to current flow across uncompensated series resistance. To measure whole-cell capacitance and series resistance, the cell was clamped at −70 mV and stepped to −65 mV for 6 ms; the resulting time-dependent current was assumed to flow across the cell's capacitance and series resistance. Only cells recorded with electrodes having a residual series resistance between 1 and 6 MΩ were included. Leak current was measured from the steady current elicited by small voltage steps (± 5 mV) from a holding potential of −75 mV during superfusion with 5–10 mM Cs^+. This study included cells with leak conductances between 0.2 and 3 nS. External Cs^+ was required to reduce the contribution of IR to the measured current. All data were analyzed and plotted using Igor Pro 2.0x (WaveMetrics, Lake Oswego, OR). A Levenberg-Marquardt, nonlinear least-squares minimization algorithm was used in the curve-fitting routines (Press et al., 1994).

RESULTS

Electrical properties of hair cells

Near the resting potential, hair cells respond to injected current with lightly damped oscillations in membrane potential at the beginning and end of the pulse (Fig. 1 *A*). Prolonged oscillations are indicative of a sharply tuned cell

TABLE 1 Composition of external solutions (mM)

	NaCl	KCl	$CaCl_2$	$MgCl_2$	HEPES	EDTA
Normal	125	4	2.2	2.8	10	—
Reduced Ca^{2+}	125	4	0.1	2.8	10	—
Buffered Ca^{2+}	110	4	1.5	8.5	5	5
	Na $MeSO_3$	K $MeSO_3$				
Reduced Cl^-	125	4	2.2	2.8	10	
	NMGCl	KCl				
Na^+-free	125	4	2.2	2.8	5	

Solutions were adjusted to pH 7.6 with NaOH (top) or NMG (bottom). Glucose (0.8 mM) was added to each solution before use. Drugs were added to normal saline, substituted for an equimolar amount of NaCl. Free Ca^{2+} concentration was measured with a Ca^{2+}-selective electrode (Microelectrodes, Inc., Bedford, NH) and adjusted to between 20 and 100 μM with 0.1 mM EDTA and 1 M $CaCl_2$.

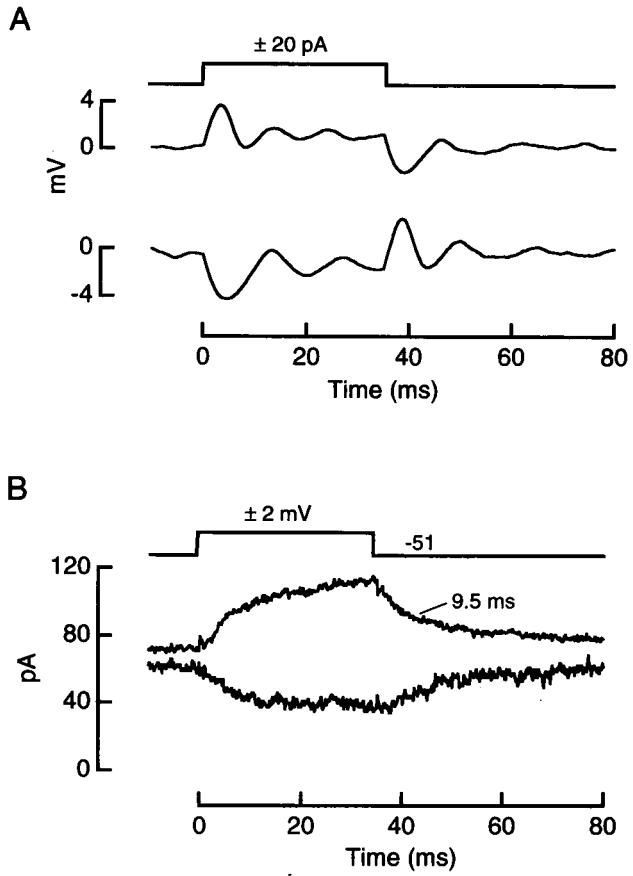

FIGURE 1 Response properties of solitary hair cells. (*A*) Membrane potential oscillation in response to 20-pA depolarizing and hyperpolarizing current steps; ordinates are relative to the resting potential of −51 mV (average of 18 and 23 presentations). Resonant frequency F_0 = 81 Hz, estimated from the average of the terminal oscillations about the resting level. The qualilty of resonance, Q_{3dB} = 2, was calculated from $Q_{3dB} = [(\pi F_0 \tau_d)^2 + 0.25]^{1/2}$, as described previously (equation 20 of Crawford and Fettiplace, 1981). (*B*) Average membrane currents for 2 mV depolarizing and hyperpolarizing pulses from the average resting potential. Outward current is plotted upward, corresponding to depolarization. Current relaxes upon repolarization with a time constant, τ = 9.5 ms (*top*). The cell capacitance, 11.5 pF, was calculated from capacity transients, which have been subtracted.

with high-quality resonance (high Q_{3dB}; see Fig. 1, *legend*), whereas a response that dies out quickly results from a broadly tuned cell with relatively low Q_{3dB}. The frequency of membrane potential oscillation, F_0, varies over two decades between cells, and in the intact papilla it is identical to the acoustic frequency to which the cell is most sensitive (Fettiplace and Crawford, 1980). In voltage clamp (Figs. 1 *B* and 2, *inset*), ionic current evoked by depolarization from the resting potential activates without a detectable instantaneous component, then decays at the end of the pulse. To a first approximation, decay is described by a single exponential function with a time constant, τ, that is related to the frequency of oscillation by $F_0 = k \cdot \tau^{-1/2}$, where k is a constant (Art and Fettiplace, 1987; Goodman, 1995; Wu et al., 1995). Previous studies have demonstrated that tail currents evoked by depolarization reverse polarity near E_K, indicating that outward current is carried chiefly by K^+ (Art and Fettiplace, 1987).

A more complete view of the hair cell *I-V* relation is shown in Fig. 2. The inset shows the whole-cell current in a 13-Hz cell held at its zero-current potential and stepped to a series of voltages between −120 and −10 mV. The steady-state *I-V* curve is similar to that obtained from hair cells in the intact ear (see figure 5 of Art et al., 1984) and shows regions of outward and inward current separated by a high-impedance region immediately hyperpolarized to the cell's resting potential. Note that the sharp outward rectification near this voltage results from the concerted action of several ionic currents, including outwardly rectifying K^+ currents; a voltage-gated Ca^{2+} current, I_{Ca} (Lewis and Hudspeth, 1983; Ohmori, 1984; Art and Fettiplace, 1987); and IR.

Behavior of IR hyperpolarized to E_K

At voltages hyperpolarized to E_K, most hair cell conductances are deactivated and the inward rectifier can be studied in isolation. Inward current activated by hyperpolarizing pulses from −60 mV in different concentrations of external K^+ are shown in Fig. 3. Many features of the hair cell IR are reminiscent of K^+-selective inward rectifiers in other cell types. First, inward current increases with an exponential time course upon hyperpolarization. The time constant is inversely related to level of hyperpolarization, but shows no systematic variation associated with resonant frequency. Second, there is a logarithmic relation between external K^+ and the peak inward current such that the maximum conductance increases in proportion to $[K^+]^n$, where n is 0.63 (Fig. 4 *A*). Third, inward current is highly selective for K^+. The reversal potential was unaffected by substituting *N*-methylglucamine for Na^+ and methanesulfonate for Cl^-, and in various external K^+, the measured values agree with those predicted for a pure K^+ conductance by the Nernst-Planck equation (Fig. 4 *B*). Fourth, a time-dependent sag is apparent in the current traces in Fig. 3, a behavior often observed in IR current records at potentials negative to −120 mV (Ohmori, 1978; Standen and Stanfield, 1979; Sakmann and Trube, 1984).

Variation in IR amplitude

Of all the IR features apparent at voltages hyperpolarized to E_K, only the maximum conductance was found to vary systematically with F_0 measured from membrane potential oscillations. As shown in Fig. 5 *A*, there is a negative correlation (R = −0.74, n = 30) between the maximum IR conductance and the cell's resonant frequency, suggesting that IR amplitude is systematically regulated. Eleven of these cells (*filled circles*) showed high-quality resonance ($Q_{3dB} > 5$) and a stronger correlation between IR size and F_0 (R = −0.89, n = 11). In general, cells containing a larger IR tended to exhibit higher quality resonance. How-

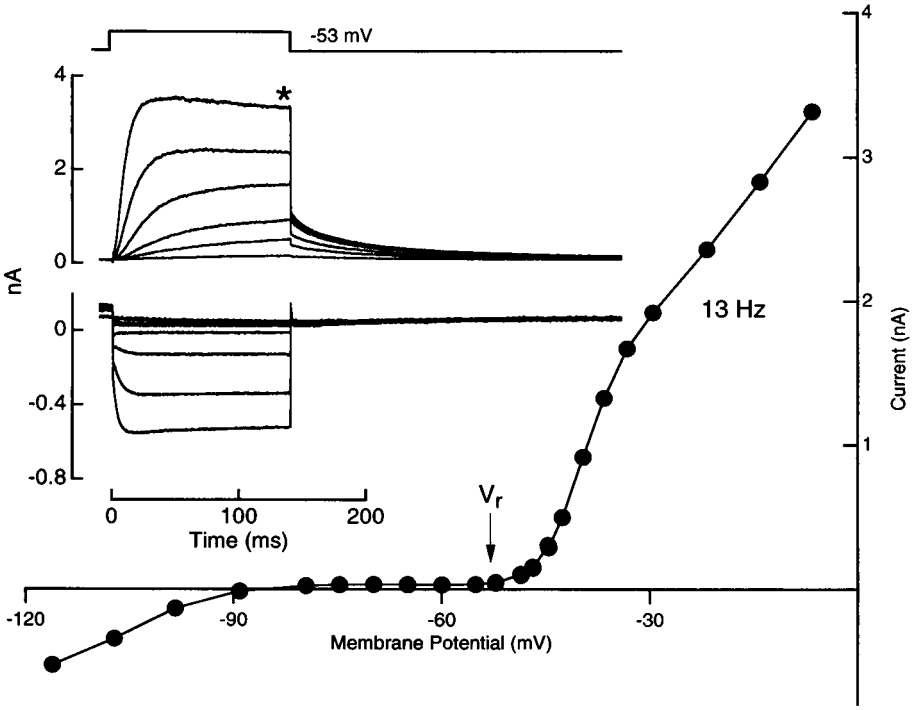

FIGURE 2 Steady-state *I-V* curves of cochlear hair cells show regions of outward and inward rectification separated by a high-impedance region. (*Inset*) Current records in a 13 Hz cell for steps from the resting potential, −53 mV. Steady-state *I-V* curves, constructed by plotting the current flowing in the last 5 ms (asterisk) of the voltage step versus membrane potential.

ever, a large IR is not sufficient by itself for high quality, because cells tuned to frequencies near 10 Hz could have large IR and $Q_{3dB} < 5$ (*open circles*). This observation implies that the contribution of IR to resonance may depend not only on its amplitude *per se*, but also on an appropriate balance with other ionic currents. Additional factors important for modifying resonant quality include an electrical shunt introduced by either the recording electrode or by activation of a voltage-independent, Ca^{2+}-activated K^+ channel present in turtle hair cells (Art et al., 1993). This latter situation is similar to the one that obtains during efferent stimulation, where addition of a linear K^+ conductance abolishes hair cell resonance (Art et al., 1984).

Isolation of IR from other ionic currents

To understand the part played by IR in electrical resonance, we devised a method for isolating IR from other ionic currents active in the voltage range covered by hair cell receptor potentials, which extend from −75 to −30 mV (Art et al., 1984). Outwardly rectifying K^+ current dominates membrane current depolarized from rest (Fig. 2) and

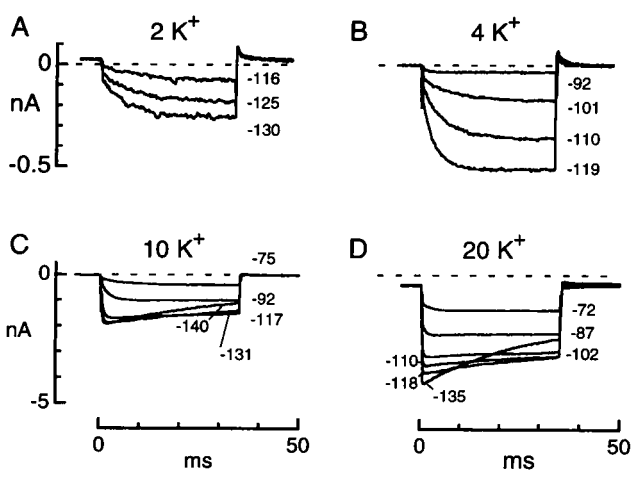

FIGURE 3 The effect of external K^+ on inward current. (*A–D*) Inward current traces for negative voltage steps from −60 mV in 2, 4, 10, and 20 mM external K^+. The voltage of each step is indicated beside each trace.

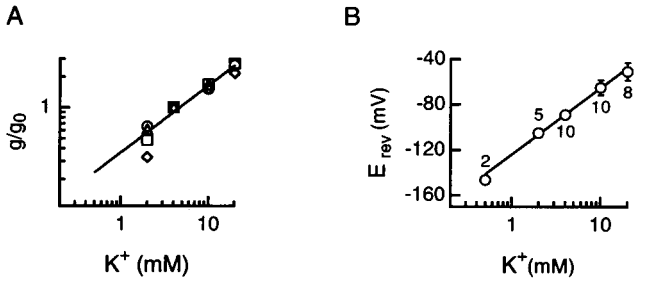

FIGURE 4 (*A*) Effect of external K^+ on maximum conductance negative to E_K. Conductance was normalized to the value in normal saline (4 mM K^+), which varied between 4.2 and 18 nS. Each symbol represents a measurement in one of four cells. The smooth line was fit to data according to the function $A[K^+]^n$, where A was 0.37 mM^{-1} and n was 0.63. Ionic selectivity of inward current. (*B*) Reversal potential versus external K^+ concentration, measured by extrapolation from the *I-V* relation for peak inward current. Bars indicate the standard deviation of the mean and are smaller than the symbols in some cases; the number of cells tested at each concentration is given beside each point. The straight line has a slope of 59 mV/decade, as predicted from the Nernst-Planck equation at T = 22°C.

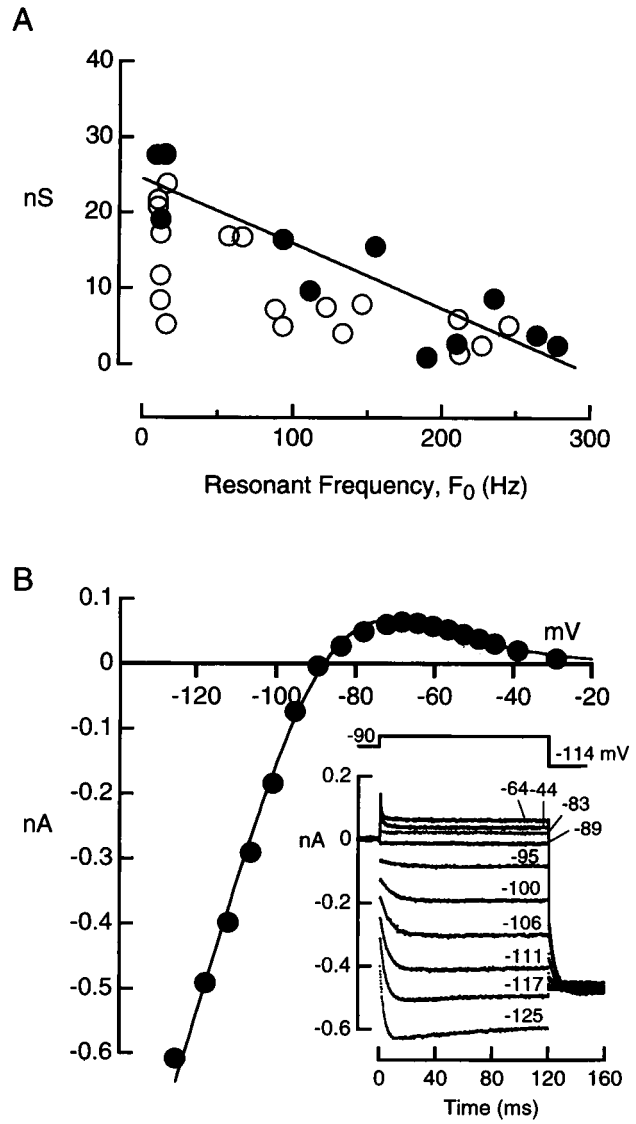

FIGURE 5 Resonant frequency and voltage dependence of IR. (*A*) IR conductance versus resonant frequency. The maximum conductance amplitude was measured negative to E_K and plotted against resonant frequency determined in current clamp from membrane potential oscillations. Filled circles (n = 11) indicate cells with high-quality resonance, $Q_{3dB} > 5$. The straight line was fit to the data for all high-quality cells (R = −0.89, n = 11) and has a slope of −0.09 nS/Hz. (*B*) Isolation of IR. Current carried by IR in a 6-Hz cell was isolated from other ionic currents by superfusing with 65 mM TEA, 5 mM 4-AP, and 50 μM nisoldipine. This cocktail blocks other ionic currents and reduces IR by 35% in a voltage-independent manner. (*Inset*) Current recorded when the cell was held at −90 mV and stepped to the potentials indicated near each trace. The *I-V* relation was constructed from peak inward current and steady-state outward current, estimated by fitting the rapid decay of the outward current with a single exponential function. Smooth curve was fit to the data using Eq. 1, with g_{max} = 18.7 nS, B = 1.05, V_B = −88 mV, V_c = 13.6 mV.

is carried predominantly by a large-conductance, Ca^{2+}-activated K^+ channel (BK) in cells tuned to more than 50 Hz (Art et al., 1995). BK is inhibited by external TEA with a half-blocking concentration (IC_{50}) of 0.21 mM (Goodman, 1995). At the lower end of the frequency spectrum, BK channels are replaced by voltage-activated K^+ channels (KVs) that are relatively insensitive to external TEA (IC_{50} = 38 mM) and exquisitely sensitive to 4-AP (IC_{50} = 20–100 μM) (Goodman, 1995). In all cells, a combination of 65 mM TEA and 5 mM 4-AP was sufficient to inhibit more than 98% of the outwardly rectifying K^+ current. The remaining current is carried chiefly by IR and dihydropyridine-sensitive voltage-gated Ca^{2+} channels. The latter can be blocked by 50 μM nisoldipine. IR thus revealed is reduced in a voltage-independent manner between −140 and −100 mV such that the conductance was decreased by 35%. The observed inhibition can be explained by the action of TEA, because superfusion with 65 mM TEA alone produced an effect of the same size (not shown). Examination of blockade at negative potentials is a good test for blockade by cation antagonists such as TEA because their efficacy, if voltage-dependent, is expected to increase with hyperpolarization. Thus, the voltage-independent blockade observed at negative potentials militates against the possibility that the composite-blocking cocktail distorts the IR current. Except where noted, IR current measured in the presence of the blocking cocktail was not corrected for the 35% reduction.

Fig. 5 *B* (*inset*) shows current recorded in the blocking cocktail in response to a series of voltage steps between −125 and −44 mV from a holding potential of −90 mV. The *I-V* curve (Fig. 5 *B*) was constructed from the peak inward current and steady-state outward current. A small, slowly activating outward current remained at potentials positive to −40 mV, and was separated from outward current carried by IR by fitting the initial rapid current relaxation with a single exponential function and assuming that the steady-state value predicted from the fitted function corresponds to outward current carried by IR. A brief pulse to −114 mV was included to further evaluate the efficacy of the blocking cocktail. At this voltage, inward current carried by IR reaches a steady level slowly compared to the time course of voltage-dependent deactivation of Ca^{2+} current, KV, and BK. Although Ca^{2+} current deactivation is too rapid to be observed, residual KV and BK could be detected as a rapidly decaying inward current superimposed on IR. Voltage steps that showed evidence of residual KV and BK were omitted from further analysis. Current carried by IR reverses polarity around E_k (−88 mV) and reaches a maximum outward current near −70 mV. At more depolarized levels, it exhibits a region of negative-slope conductance contained entirely within the physiological voltage range.

Voltage dependence of IR

As a framework for examining the voltage dependence of IR in cells tuned to different frequencies, Eq. 1 was derived from a model of inward rectification developed fully in the Appendix. Briefly, the model assumes that between −110 and 0 mV, the inward rectifier behaves as constant conductance subject to voltage-dependent block by an unknown intracellular particle. Current-voltage curves such as the one in Fig. 5 *B* can be described by

$$I = g_{max} \cdot (V - E_K) \frac{1}{1 + B \exp((V - V_B)/V_e)}, \quad (1)$$

where g_{max} is the maximum conductance negative to E_K and was assigned by measurement of peak inward currents, V_B is the midpoint for block, and V_e is the voltage dependence of the block. B is a dimensionless constant defined as

$$B = [\beta]_i / K_B, \quad (2)$$

with $[\beta]_i$ equal to the blocking particle concentration, and K_B, its apparent dissociation constant at V_B. Five cells with g_{max} between 6.3 and 18.7 nS were used to estimate the parameters B, V_B, and V_e by fitting current-voltage relations similar to the one shown in Fig. 5 *B* to Eq. 1 (Table 2). Parameter values were similar in all cells and independent of g_{max}, suggesting that hair cells differ only in the level of expression of IR. Therefore, the amplitude of g_{max} hyperpolarized to E_K is an accurate predictor of IR outward current in the vicinity of the resting potential. Because the maximum IR conductance is inversely related to F_0 (Fig. 5 *A*), the contribution of IR to the total resting conductance and its part in setting the resting potential must also be frequency dependent.

Behavior in the negative-slope region

A detailed examination of the decrease in outward current in the negative-slope region of the steady-state *I-V* curve reveals the full import of IR. Fig. 6 *A* shows current traces for small depolarizations from a holding potential of −57 mV. A new steady level was achieved after an exponential time course in less than 2.5 ms. The time constant was modestly voltage sensitive (Fig. 6 *B*) and did not appear to vary to between cells tuned to different frequencies (n = 3). The rapid kinetics displayed by IR near the resting potential indicate that it is unlikely to contribute to the kinetics of the net current (see Figs. 1 *B* and 2, *inset*) and, hence, does not play a role in determining resonant frequency. Fig. 6 *C* compares the negative-slope region of IR for a cell tuned to 10 Hz with the steady-state voltage dependence of the Ca^{2+} current for cells at this frequency (see Wu et al., 1995) and shows that the combined effect of IR and the Ca^{2+} current is to provide positive feedback over the range −70 to −20 mV, a feature that enhances excitability in general and resonant quality in particular (Ashmore and Attwell, 1985; Fettiplace, 1987; Hudspeth and Lewis, 1988).

Effect of external K^+ on the steady-state *I-V* curve

As shown in Fig. 4, variation of external K^+ affects the reversal potential and the maximum IR conductance hyperpolarized to E_K (g_{max}). Examining IR in elevated external K^+ also reveals changes in the *I-V* relation in the physiological voltage range. The experiment was similar to the one shown in Fig. 5. Cells were superfused with the blocking cocktail containing either normal (4 mM) or elevated (10 mM) K^+ (Fig. 7 *A*). The effects were quantified by fitting the current-voltage curves with Eq. 1 and comparing the fitting parameters in normal and elevated K^+ (n = 3, Table 2). Apart from the expected increase in g_{max} (see Fig. 4 *A*), the main effect is to reduce B, which is equal to the concentration of the intracellular blocking particle, $[\beta]_i$, divided by the apparent dissociation constant, K_B, at V_B (Eq. 2). Because $[\beta]_i$ is unlikely to change during the course of an experiment, a reduction in B implies that raising external K^+ increases K_B and lowers the affinity of IR for the blocking particle, a result consistent with the view that external K^+ exerts its effect on IR by interacting with the particle in the pore (Hille and Schwarz, 1978). The relation between B and external $[K^+]$ was further evaluated by fitting steady-state *I-V* curves in 2 and 4 mM K^+ in two other cells. Fig. 7 *B* shows that B varies in proportion to $[K^+]^{-m}$, where m is 1.5. This empirical relation, the mean fitting parameters given in Table 2, and the relation between external K^+ and the maximum conductance (Fig. 4 *A*) were used to calculate the *I-V* curves in Fig. 7 *C*. They illustrate that outward current carried by IR at the hair cell resting potential (*arrows*) increases as external K^+ is increased, despite a reduction in the driving force for outward current. In addition, the extent of positive feedback is determined by a shift in the voltage range over which a negative slope is observed in the steady-state *I-V* curve. As shown in Fig. 7 *C*, at the resting potential of −50 mV the negative slope conductance is at maximum in normal (4 mM) K^+.

TABLE 2 IR steady-state voltage dependence in 4 mM and 10 mM external K^+

	4 mM K^+				10 mM K^+			
F_0' (Hz)	B	V_B (mV)	V_e (mV)	g_{max} (nS)	B	V_B (mV)	V_e (mV)	g_{max} (nS)
12	1.56	−87	8.16	10.9	0.34	−87	10.9	21.5
10	1.22	−89	12.6	6.29	—	—	—	—
7	1.67	−88	10.6	15.3	0.50	−81	11.3	35.9
6	1.05	−88	13.6	18.7	—	—	—	—
3	1.57	−90	11.0	13.9	0.31	−93	12.2	29.1

Fitting parameters of inward rectification are defined by Eq. 1. For fits in 4 mM K^+, E_K was taken as −88 mV. Mean (±SD) values for B, V_B, and V_e were 1.41 (±0.27), −88 (±1) mV, and 11.2 (±2.1) mV. For fits in 10 mM K^+, E_K was taken as −68 mV. Mean (±SD) values for B, V_B, and V_e were 0.38 (±0.27), −87 (±6) mV, and 11.5 (±0.7) mV.

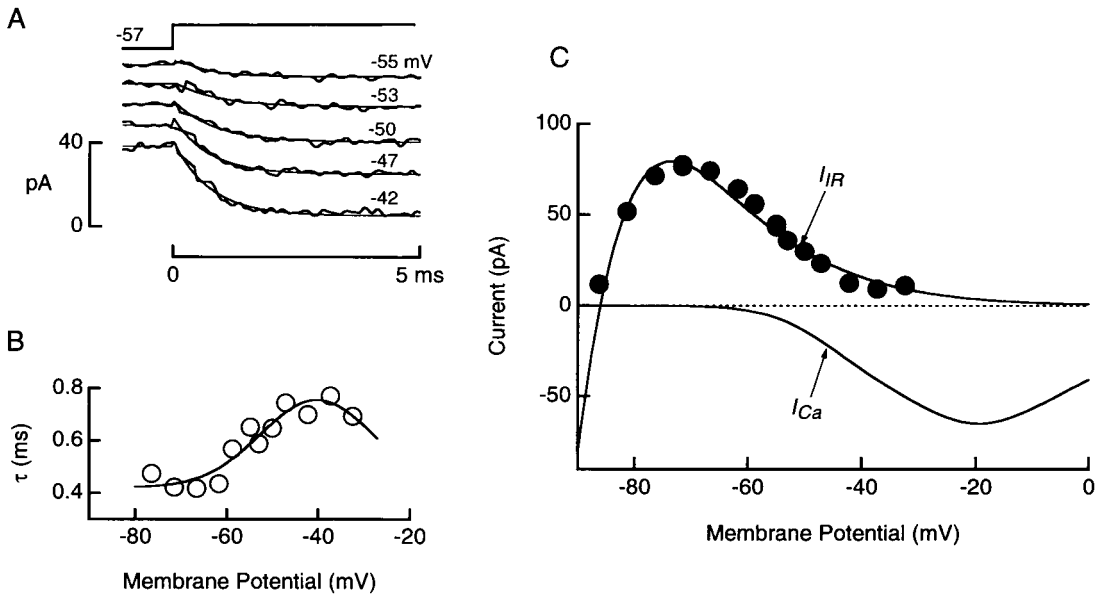

FIGURE 6 Behavior of IR in the physiological voltage range. (*A*) Rapid block produced by small depolarizations from −57 mV. Current carried by IR was isolated using 65 mM TEA, 5 mM 4-AP, and 50 μM nisoldipine. Each trace is the average of four to six presentations and was digitally filtered with a three-point Gaussian filter. Single exponential functions (thin lines) were fit to the onset of the block. (*B*) Time constant, τ, of IR block exhibits a modest voltage sensitivity about the resting level. (*C*) Comparison of the negative slope region of IR with the average calcium *I-V* curve. Filled symbols are the steady-state current measured in the blocking cocktail, scaled to account for 35% inhibition of IR. Smooth curve was calculated using Eq. 1, with fitting parameters: g_{max} = 35 nS, E_K = −86 mV, B = 2.0, V_B = −88 mV, V_c = 11 mV. Calcium current was calculated following the method of Wu et al. (1995), according to $I_{Ca} = Ni_{Ca}p_{Ca}$, where N is the number of channels, i_{Ca} is the single-channel current given by the constant field equation, and p_{Ca} is the steady-state open probability, calculated from an m^2 Hodgkin-Huxley scheme. N was adjusted to give the peak I_{Ca} estimated from the relation between Ca^{2+} current size and F_0 determined previously (Art et al., 1993).

Inhibition of IR by external cations

To demonstrate the contribution of IR to electrical resonance in current clamp, it was necessary to identify a selective blocker of the hair cell IR. External Ba^{2+} and Cs^+ were good candidates, because micromolar concentrations inhibit inward current carried by K^+-selective inward rectifiers in other cell types. Like an IRK1 homolog cloned from the chick cochlea (Navaratnam et al., 1995), IR in turtle hair cells was relatively insensitive to inhibition by Ba^{2+} ($IC_{50} \approx 150$ μM at −100 mV). The effect of Ba^{2+} was not tested further, because the millimolar concentrations required to block IR would also affect BK and the voltage-gated Ca^{2+} current (Art and Fettiplace, 1987). In contrast, 5 mM external Cs^+ blocks little if any of these currents, producing at most a 1–2% reduction, while producing a 92% block of IR at −100 mV.

The Cs^+ blockade of IR was highly voltage dependent, however, showing its greatest effect at negative potentials (Fig. 8 *A*). To determine what fraction of IR was blocked by 5 mM Cs^+ near the resting potential, the inhibition constant, K_i, was measured by constructing dose-response curves at several potentials (Fig. 8 *B*). These were best described by binding curves with different Hill coefficients, which ranged from 0.99 to 2.3 and increased with depolarization. Fig. 8 *C* shows K_i measured at several potentials (n = 3), and fitted according to Woodhull's model of voltage-dependent blockade. The equivalent electrical distance, δ, derived from this analysis was 1.9, suggesting the presence of multiple binding sites within the membrane electrical field. Similar values have been reported for cloned IRK1 channels (Kubo et al., 1993) and for K^+-selective inward rectifiers in frog saccular hair cells (Holt and Eatock, 1995) and tunicate oocytes (Hagiwara et al., 1976). It is important to note that Cs^+ inhibits outward current carried by IR, albeit with low affinity, and that inhibition of outward current is described by the same function of voltage that obtains for inward current. Therefore, it seems likely that inhibition results from a single mechanism at all potentials wherein Cs^+ binds to the ion pore and prevents permeation by K^+.

Effect of external Cs^+ on resonance

In cells tuned to <30 Hz, superfusion with saline containing 5 mM Cs^+ converted membrane potential oscillations evoked by current injection into highly damped depolarizations. An example is illustrated in Fig. 9 *A*, which shows that external Cs^+ reversibly abolished resonance in a 20-Hz cell. As expected for inhibition of an outward current, a modest (~2.5 mV) depolarization was observed. These effects are likely to result from partial inhibition of outward current carried by IR. Support for this idea includes the following. First, IR is the primary target for inhibition by external Cs^+ between −75 and −30 mV. Second, the relation between K_i and voltage (Fig. 8 *C*) predicts that 5

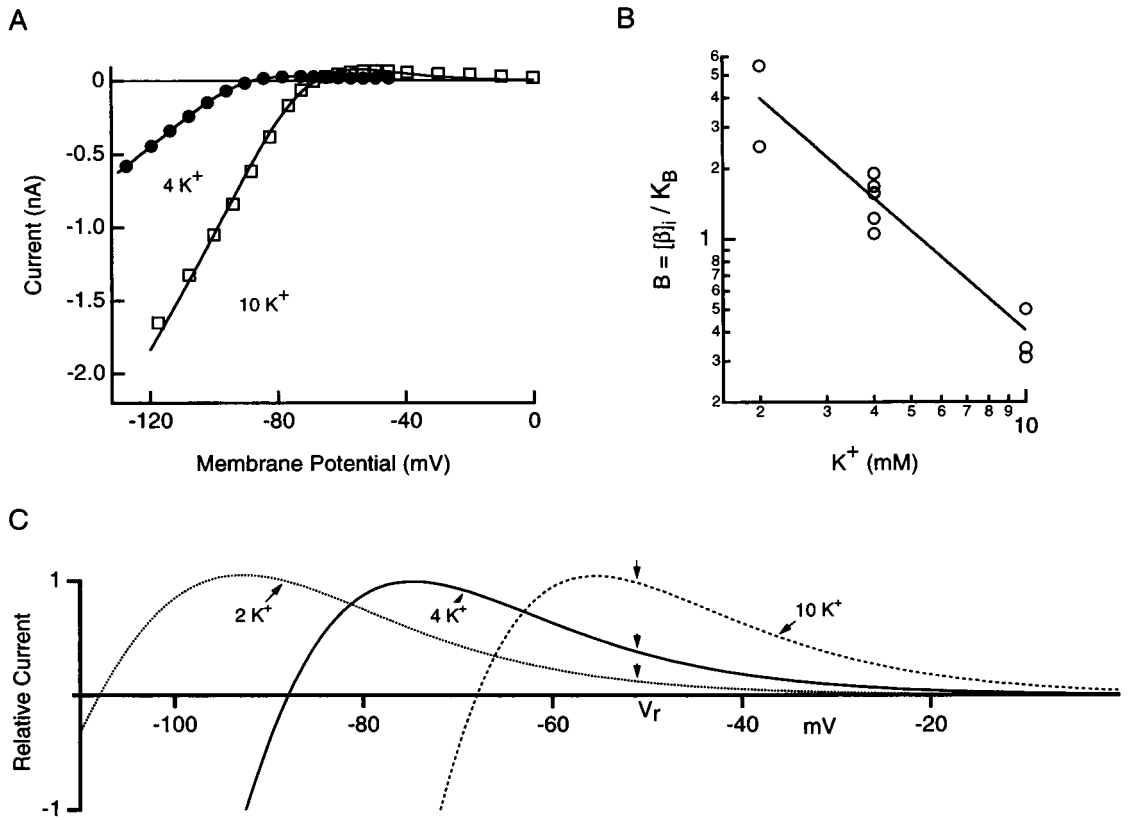

FIGURE 7 The effect of elevated external K^+ on IR in a 7-Hz cell. (*A*) Steady-state current measured as described for Fig. 5 *B*, except that the cell was voltage-clamped at −70 mV in 10 mM K^+. A small Ca^{2+} current remained in this recording (10 pA at 20 mV) and was subtracted from the measured current using the voltage dependence measured previously (Art et al., 1993). (*B*) The fitting parameter, *B*, depends on external K^+. Values for *B* were estimated by fitting steady-state *I-V* curves with Eq. 1. Three cells were tested in 4 and 10 mM K^+ and two cells were tested in 2 and 4 mM K^+. The straight line was fit to the data according to $B = C[K^+]^{-m}$, where *C* was 11 mM^{-1} and *m* was 1.5. (*C*) Modulation of steady-state *I-V* by external K^+. *I-V* curves in 2, 4, and 10 mM K^+ were calculated using Eq. 1 and normalized to give a maximum outward current of 1 in normal (4 mM K^+) saline. Arrows indicated the average resting potential (−50 mV). Values for g_{max} and *B* were calculated from the curve fits given in Figs. 4 *B* and 7 *B*, respectively. The other parameters were the mean values given in Table 1.

mM Cs^+ blocks ~25% of IR at −50 mV. It should be noted that Q_{3dB} is steeply voltage dependent and, in the turtle cochlea, reaches its maximum value near the average resting potential of −50 mV (Crawford and Fettiplace, 1980). Therefore, changes in electrical resonance could result from depolarization, diminished positive feedback, or both. The contribution of membrane voltage was investigated by injecting sufficient current into the cell in Fig. 9 *A* to produce a 3-mV depolarization from the voltage of maximum Q_{3dB}. This maneuver decreased Q_{3dB} to approximately half of its maximum value as compared to a ~4-fold reduction during superfusion with Cs^+, a result which suggests that depolarization alone is not sufficient to explain its effects. The relative importance of membrane voltage and IR for determining Q_{3dB} was explored further by testing the effects of external Cs^+ in cells tuned to higher frequencies. In a 68-Hz cell (Fig. 9 *B*), external Cs^+ reduced Q_{3dB} by a factor of ~4 without significantly affecting resonant frequency and depolarized the cell by about 0.5 mV. A 1-mV depolarization (by current injection) increased resonant quality by ~5-fold (not shown), confirming that the Cs^+-dependent reduction in Q_{3dB} cannot be attributed to depolarization.

The effect of Cs^+ superfusion on resonant quality was further quantified by calculating a *Q* ratio defined by the following relation:

$$Q \text{ ratio} = \frac{(Q - Q_{min})}{(Q_{Cs} - Q_{min})}. \quad (3)$$

where *Q* is resonant quality measured in normal saline, Q_{Cs} is the quality measured during superfusion with 5 mM Cs^+, and Q_{min} has a value of 0.5 and is the theoretical minimum quality produced by assuming a decay time constant of zero for membrane potential oscillations. The value of Q_{min} arises naturally from the calculation of Q_{3dB} from damped oscillations in membrane voltage (see Fig. 1). A *Q* ratio of 1 indicates a cell in which Cs^+ had no effect on resonance. Fig. 10 (*top*) shows that the *Q* ratio declines with resonant frequency. A parallel relation between IR size and frequency is evident in the same cells (Fig. 10, *bottom*). This result indicates that the effect of external Cs^+ on Q_{3dB} depends not only on resonant frequency, but also on IR size and provides additional support for the conclusion that the observed reduction in Q_{3dB} results from blockade of IR. In

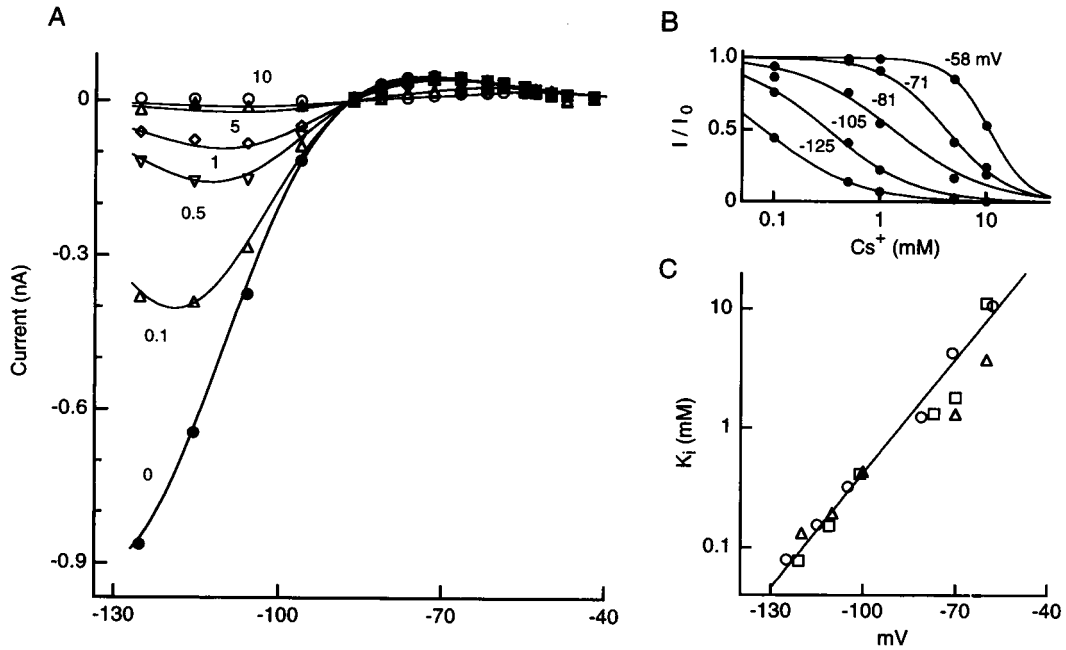

FIGURE 8 Voltage dependence of Cs^+ block. (*A*) Inhibition of IR by external Cs^+. Steady-state current-voltage curve in normal 65 mM TEA, 5 mM 4-AP, and 50 μM nisoldipine in the presence of increasing concentrations of Cs^+ (in mM), as indicated near each curve. The smooth curve through the data in the absence of Cs^+ is given by the product of Eq. 1 and a Boltzmann function, $1/(1 + \exp((V + 140)/12))$, which accounts for the apparent decrease in conductance hyperpolarized to -110 mV. The parameters used in Eq. 1 were $g_{max} = 32.6$ nS, $B = 1.91$, $V_B = -92$ mV, $V_e = 12.7$ mV. (*B*) Dose-response relations at several potentials. Current was expressed relative to the current measured in the absence of Cs^+ (I_0) from the *I-V* curves in *A*, and the inhibition constant, K_i, was measured by fitting the dose-response curve at each voltage with a Hill equation, $I/I_0 = 1 - \{[Cs^+]^n/(K_i^n + [Cs^+]^n)\}$. The value of n increased with voltage, ranging from 0.99 at -125 mV to 2.33 at -58 mV. (*C*) Collected results for three cells. K_i for Cs^+ was measured at membrane potentials ranging from -130 to -60 mV. The smooth line is fit according to $K_i = K(0) \exp(\delta zFV/RT)$, where $K(0)$ is the inhibition constant at 0 mV; δ is the equivalent electrical distance; z is the valence; F is the Faraday constant; R is the universal gas constant; and T is 22°C. The fit gave values of 0.79 M for $K(0)$ and 1.9 for δ.

addition, we find that a reduction in IR is tolerated by cells tuned to higher frequencies. Because these cells exhibit high-quality resonance, the functional role of IR may be supplanted by another current. One candidate is the voltage-gated Ca^{2+} current, whose amplitude increases with F_0 (Art and Fettiplace, 1987; Art et al., 1993). The contribution of I_{Ca} to high-quality resonance has been considered previously (Ashmore and Attwell, 1985; Hudspeth and Lewis, 1988) and relates to both the role of Ca^{2+} in gating BK channels and positive feedback conferred by the time and voltage dependence of the ionic current. Both IR and I_{Ca} have the time and voltage dependence expected of an ionic current responsible for positive feedback (Fig. 6 *C*), and, although they operate over different voltage ranges, both currents may be viewed as enhancing resonant quality.

DISCUSSION

IR function in hair cells

Although previous studies of hair cells have noted the existence of an inward rectifier (Ohmori, 1984; Art and Fettiplace, 1987; Fuchs and Evans, 1990) and proposed that IR establishes a hyperpolarized resting potential (Holt and Eatock, 1995), a part for IR in electrical resonance was considered unlikely because it carries large currents hyperpolarized to the voltage range covered by hair cell receptor potentials (Art and Fettiplace, 1987). However, after isolating IR from other ionic currents active within this voltage range, we find that it generates positive feedback and, therefore, serves an electrical function similar to activation of the voltage-gated Ca^{2+} current. This is illustrated by considering the sequence of ionic events that occur in response to current injection. Depolarization leads to rapid inhibition of IR and activates the Ca^{2+} current. The response of both IR and I_{Ca} to depolarization provides positive feedback (see Fig. 6 *C*), tending to depolarize the cell further. After a delay, the outwardly rectifying K^+ currents, KV and BK, repolarize the cell toward its original resting level. As the cell hyperpolarizes, outward current carried by IR increases and I_{Ca} deactivates (see Fig. 6 *C*). The cell's membrane potential momentarily dips below its mean level as a result of delays inherent in deactivating BK and KV. A similar sequence of events obtains for an acoustic stimulus that produces a sinusoidal deflection of the hair bundle and thereby modulates transducer current. A large, oscillatory receptor potential ensues if the sound frequency is appropriate for the kinetics of the outwardly rectifying currents in a given cell.

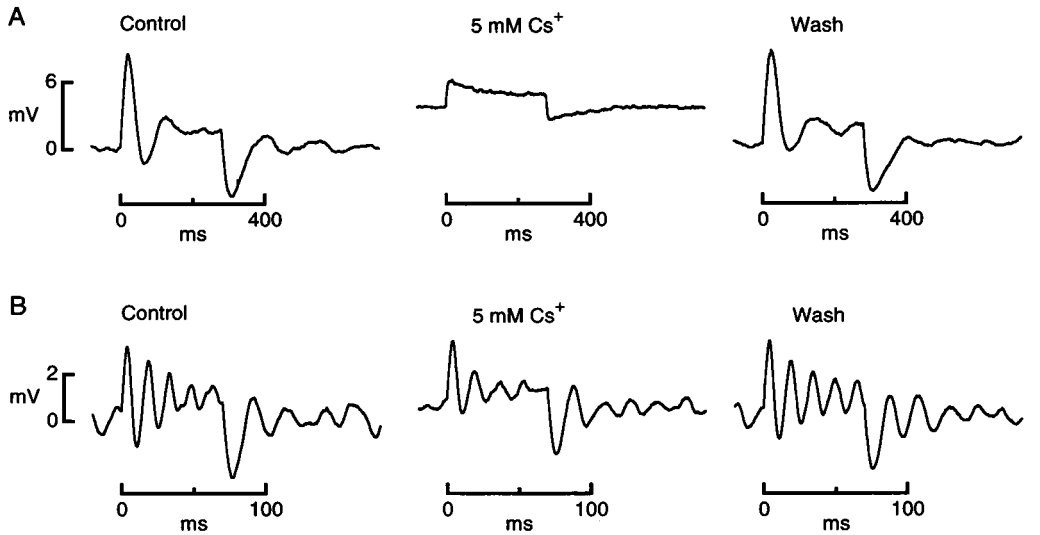

FIGURE 9 Reversible effect of external Cs^+ on electrical resonance of hair cells in current clamp. The two cells illustrated were tuned to low and middle frequencies, but had similar values for g_{max}. (*A*) Damped oscillations of a 20-Hz cell (g_{max} = 19 ns) in response to a 20-pA, 280-ms current step in normal saline (Control) and in saline containing 5 mM Cs^+. Resonance returned after removing Cs^+ (Wash). Q_{3dB} was 2.1 before (Control) and 1.5 after (Wash) exposure to Cs^+. (*B*) Damped oscillations of a 68-Hz cell (g_{max} = 16 nS) in response to a 50-pA current step before, during, and after superfusion with saline containing 5 mM Cs^+. Q_{3dB} was 9.2 (Control), 2.2 (5 mM Cs^+), and 8.4 (Wash). Between 20 and 50 presentations were averaged to form each trace.

It is convenient to think of IR and I_{Ca} as two rapidly acting, regenerative currents operating in overlapping voltage ranges and having similarly steep negative slopes (Fig. 6 *C*). The comparison is appropriate given that IR inhibition increases *e*-fold in 11 mV (Table 1) and I_{Ca} activates *e*-fold in 8 mV (Art et al., 1993). One consequence of having IR is to extend the voltage range over which positive feedback is generated to −75 mV without the increased ionic load that would accompany a hyperpolarizing shift in the voltage dependence of the Ca^{2+} current or inclusion of a voltage-gated Na^+ current. The functional similarity between IR and I_{Ca} is strengthened by the observation that both IR inhibition (Fig. 6 *B*) and I_{Ca} activation (Art and Fettiplace, 1987) have time constants of a few hundred microseconds near the resting potential. However, the relative importance of IR and I_{Ca} for high-quality electrical resonance is likely to vary with F_0 because the size of both currents is frequency dependent. In particular, the size of I_{Ca} increases (Art and Fettiplace, 1987; Art et al., 1993) whereas the size of IR declines with F_0. This expression pattern may account, at least in part, for the observation that IR is required for resonance in cells having the smallest Ca^{2+} current, those tuned to low frequencies (Fig. 9 *A*).

IR function in other excitable cells

Potassium-selective inward rectifiers are effective tools for stabilizing membrane potential because the open probability at membrane voltages typical of resting nerve and muscle is large compared to that of other ionic conductances. In the event that IR is the dominant conductance active at rest, it will tend to hold the membrane voltage near E_K, oppose modest depolarizations, and decrease excitability. Demonstrating that IR plays a significant role in hair cell resonance indicates that inward rectifiers may also act to increase excitability by generating positive feedback. The choice between the two roles depends on membrane potential. IR generates positive feedback in any cell whose membrane potential is depolarized compared to the voltage at which outward current carried by IR reaches a peak (roughly −70 mV in hair cells). Feedback strength will depend on IR amplitude and the degree of inward rectification. This is particularly interesting in light of the observation that K^+-selective inward rectifiers may contribute to signal transduction in neurons and endocrine cells in which current amplitude is regulated by G proteins (Bauer et al., 1990; Yamaguchi et al., 1990; Inoue and Imanaga, 1993; Pennington et al., 1993; Farkas et al., 1994). Consider also the observation that the steepness of the negative slope region in IRK1 depends on polyamine and Mg^{2+} concentration at the channel's internal face (Lopatin et al., 1994; Fakler et al., 1995), raising the possibility that the feedback strength is a dynamic function of their intracellular concentration.

Steady-state voltage dependence of IR

We have modeled the voltage dependence of IR as a constant conductance, blocked at depolarized potentials by an intracellular blocking particle. This model is sufficient to describe the steady-state voltage dependence of IR, including its behavior within the voltage range important for hair cell function, and suggests a few simple methods for modifying its voltage dependence. In particular, the fitting parameter, *B*, may be altered

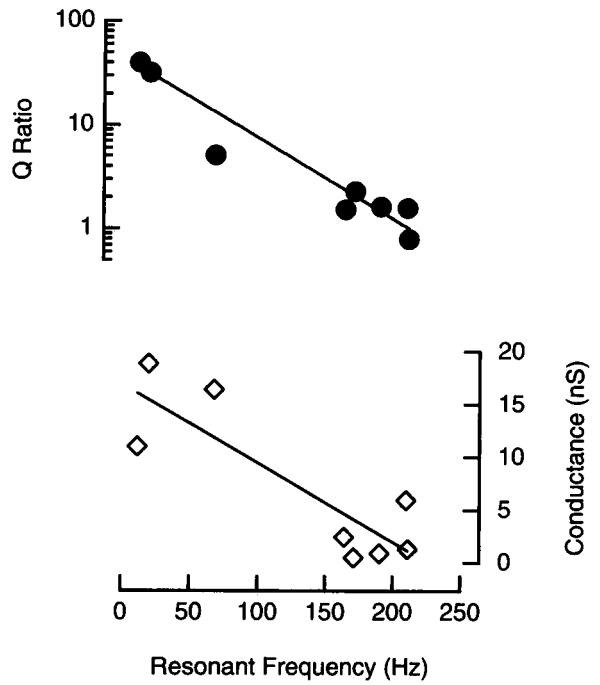

FIGURE 10 External Cs^+ reduces resonant quality in a frequency-dependent manner. (*Top*) Q_{3dB} was measured in current clamp in normal saline and during superfusion with saline containing 5 mM Cs^+. The effect on Q_{3dB} was quantified by calculating a Q ratio from $(Q - Q_{min})/(Q_{Cs} - Q_{min})$, where Q_{min} has a value of 0.5 and corresponds to membrane potential oscillations that decay with a zero time constant (see Fig. 1 legend for definition of Q). Smooth line drawn by eye. (*Bottom*) IR conductance versus F_0 in the same cells. Smooth line was fit to the data ($R = -0.86$, $n = 8$).

by changing the concentration of the intracellular blocking particle, its apparent dissociation constant for binding to the channel, or both (Eq. 2). Variations in external K^+ affect the negative slope region, as illustrated in Fig. 7 *C* for different values of *B* estimated in 2, 4, and 10 mM K^+. Two effects are apparent at the hair cell resting potential: 1) outward current increases with K^+; and 2) the negative slope is steepest in 4 mM K^+. Both of these effects arise largely as a consequence of the K^+ dependence of *B* (Eq. 1, Fig. 7 *B*). These observations raise the possibility that IR's contribution to membrane current in the physiological voltage range and its ability to generate positive feedback may be actively controlled *in vivo* by activity-dependent accumulation of external K^+ (e.g., Neher and Lux, 1973). The tendency for variations in external K^+ to arise would be accentuated in the presence of a diffusion barrier such as that imposed by a myelin sheath, a closely packed epithelium, or a calyceal nerve ending such as that encasing type I vestibular hair cells (Wersäll, 1956).

Experimental evidence in support of the idea that inward rectification results from voltage-dependent blockade by an intracellular particle has been obtained in single-channel experiments showing that rectification is relieved by removing internal Mg^{2+} from native (Vandenberg, 1987; Matsuda, 1988) and cloned inward rectifiers (Nichols et al., 1994; Stanfield et al., 1994b). Two polyamines, spermine and spermidine, were also identified as potential blocking particles because they produce high-affinity blockade of outward current carried by IRK1 channels (Ficker et al., 1994; Lopatin et al., 1994; Fakler et al., 1995). It is possible that polyamines function as blocking particles in hair cells, because spermine, spermidine, and ornithine decarboxylase, the initial enzyme for their synthesis, are present in the vertebrate cochlea (Schweitzer et al., 1986; Henley et al., 1987). In addition, they appear to be important for auditory function, because treatment with α-difluoromethylornithine, an irreversible inhibitor of ornithine decarboxylase, raises the threshold for brainstem auditory responses in guinea pigs (Salzer et al., 1990) and induces a reversible hearing loss in a significant portion of cancer patients receiving this drug as part of a chemotherapy regimen (Abeloff et al., 1986).

APPENDIX: MODEL OF INWARD RECTIFICATION

A simple description of hair cell inward rectification was derived by assuming that the underlying conductance is constant between −110 and 0 mV, and subject to a voltage-dependent block by an unknown intracellular particle. We consider the underlying binding reaction:

$$\beta + O \underset{\kappa}{\overset{\mu}{\rightleftarrows}} \beta O, \tag{4}$$

where O denotes a conducting (unblocked) channel and βO is nonconducting (blocked), and κ and μ are voltage-dependent rate constants.

In the steady state, the probability, p, that the channel is unblocked at any voltage can be found by setting

$$dp/dt = (1 - p)\kappa - p\mu[\beta]_i = 0, \tag{5}$$

which yields

$$p_\infty = \kappa/(\kappa + \mu[\beta]_i). \tag{6}$$

We assume that the apparent dissociation constant, given by the ratio of the backward and forward rate constants, has a voltage dependence of the form

$$\kappa/\mu = K_B \exp\{(V - V_B)/V_e\}, \tag{7}$$

where K_B is the apparent dissociation constant at V_B. If V_B is 0 mV, then the equation reduces to Woodhull's model of voltage-dependent inhibition of Na^+ current by external protons. An attempt to fit IR *I-V* curves by fixing V_B to 0 mV gave unsatisfactory results, especially in the degree of curvature approaching the maximum outward current and in the voltage for maximum outward current, which was generally more positive than found experimentally.

Substitution of the voltage dependence of the apparent dissociation constant into the equation for steady-state open probability yields

$$p_\infty = 1/\{1 + ([\beta]_i/K_B) \exp((V - V_B)/V_e)\}. \tag{8}$$

The current due to the inward rectifier is given by

$$I = g_{max} \cdot (V - E_K) \cdot p_\infty, \tag{9}$$

or,

$$I = g_{max} \cdot (V - E_K) \frac{1}{1 + ([\beta]_i/K_B) \exp((V - V_B)/V_e)}, \tag{10}$$

where g_{max}, the maximum conductance hyperpolarized to E_K, is assumed to be the product of the number of channels and the unitary conductance. For convenience, we define a constant $B = [\beta]_i/K_B$ and substitute into Eq. 10 to yield Eq. 1 of the text.

Nisoldipine was the kind gift of Bayer Pharmaceutical Division (West Haven, CT). We thank H. Denison and S. Wen for their technical assistance and R. Fettiplace, S. Nakajima, Y. Nakajima, and D. Nelson for comments on the manuscript.

This work was supported by National Institutes of Health grant DC00454, an A. P. Sloan Fellowship, a Brain Research Foundation grant to JJA, and a Howard Hughes Predoctoral Fellowship to MBG.

REFERENCES

Abeloff, M. D., S. T. Rosen, G. D. Luk, S. B. Baylin, M. Zeltzmann, and A. Sjoerdsma. 1986. Phase II trials of α-difluromethylornithine, an inhibitor of polyamine synthesis, in advanced small cell lung cancer and colon cancer. *Cancer Treat. Rep.* 70:843–845.

Art, J. J., and R. Fettiplace. 1987. Variation of membrane properties in hair cells isolated from the turtle cochlea. *J. Physiol. (Lond.).* 385:207–242.

Art, J. J., R. Fettiplace, and P. A. Fuchs. 1984. Synaptic hyperpolarization and inhibition of turtle cochlear hair cells. *J. Physiol. (Lond.).* 356: 525–550.

Art, J. J., R. Fettiplace, and Y.-C. Wu. 1993. The effects of low calcium on the voltage-dependent conductances involved in tuning of turtle hair cells. *J. Physiol. (Lond.).* 470:109–126.

Art, J. J., Y.-C. Wu, and R. Fettiplace. 1995. The calcium-activated potassium channels of turtle hair cells. *J. Gen. Physiol.* 105:49–72.

Ashmore, J. F., and D. Attwell. 1985. Models for electrical tuning in hair cells. *Proc. R. Soc. Lond. B.* 226:325–344.

Bauer, C. K., W. Meyerhof, and J. Schwarz. 1990. An inward-rectifying K^+ current in clonal rat pituitary cells and its modulation by thyrotrophin-releasing hormone. *J. Physiol. (Lond.).* 429:169–189.

Corey, D. P., and A. J. Hudspeth. 1979. Ionic basis of the receptor potential in a vertebrate hair cell. *Nature.* 281:675–677.

Crawford, A. C., and R. Fettiplace. 1980. The frequency selectivity of auditory nerve fibers and hair cells in the cochlea of the turtle. *J. Physiol. (Lond.).* 306:377–412.

Crawford, A. C., and R. Fettiplace. 1981. An electrical tuning mechanism in turtle cochlear hair cells. *J. Physiol. (Lond.).* 312:377–412.

Fakler, B., U. Brändle, E. Glowatzki, S. Weidemann, H.-P. Zenner, and J. P. Ruppersberg. 1995. Strong voltage-dependent inward rectification of inward rectifier K^+ channels is caused by intracellular spermine. *Cell.* 80:149–154.

Farkas, R. H., S. Nakajima, and Y. Nakajima. 1994. Neurotensin excites basal forebrain cholinergic neurons: ionic and signal-transduction mechanisms. *Proc. Natl. Acad. Sci. USA.* 91:2853–2857.

Fettiplace, R. 1987. Electrical tuning in hair cells. *Trends Neurosci.* 10: 421–425.

Fettiplace, R., and A. C. Crawford. 1980. The origin of tuning in turtle cochlear hair cells. *Hear. Res.* 2:447–454.

Ficker, E., M. Taglialatela, B. A. Wible, C. M. Henley, and A. M. Brown. 1994. Spermine and spermidine as gating molecules for inward K^+ channels. *Science.* 266:1068–1072.

Fuchs, P. A., and M. G. Evans. 1990. Potassium currents in hair cells isolated from the cochlea of the chick. *J. Physiol. (Lond.).* 429:529–551.

Goodman, M. B. 1995. A functional analysis of potassium currents in turtle cochlear hair cells. Ph.D. dissertation. The University of Chicago.

Goodman, M. B., and J. J. Art. 1993. Effects of external cesium on the voltage-dependent conductances involved in tuning of turtle hair cells. *Soc. Neurosci. Abstr.* 19:1538.

Hagiwara, S., S. Miyazaki, and N. P. Rosenthal. 1976. Potassium current and the effect of cesium on this current during anomalous rectification of the egg cell membrane of a starfish. *J. Gen. Physiol.* 67:621–638.

Hamill, O. P., A. Marty, E. Neher, B. Sakmann, and F. J. Sigworth. 1981. Improved patch-clamp techniques for high-resolution current recording from cells and cell-free membrane patches. *Pflugers Arch.* 391:85–100.

Henley, C. M., H. J. Gerhardt, and J. Schacht. 1987. Inhibition of inner ear ornithine decarboxylase by neomycin in vitro. *Brain Res. Bull.* 19: 695–698.

Hille, B. 1992. Ionic Channels of Excitable Membranes. Sinauer, Sunderland, MA.

Hille, B., and W. Schwarz. 1978. Potassium channels as multi-ion single-file pores. *J. Gen. Physiol.* 72:409–442.

Holt, J. R., and R. A. Eatock. 1995. Inwardly rectifying currents of saccular hair cells from the leopard frog. *J. Neurophysiol.* 73:1484–1502.

Hudspeth, A. J., and R. S. Lewis. 1988. A model for electrical resonance and frequency tuning in saccular hair cells of the bullfrog, *Rana catesbiana. J. Physiol. (Lond.).* 400:275–297.

Inoue, M., and I. Imanaga. 1993. G protein-mediated inhibition of inwardly rectifying K^+ channels in guinea pig chromaffin cells. *Am. J. Physiol.* 265 (*Cell Physiology* 34): C946–C956.

Krishtal, O. A., and V. I. Pidoplichko. 1980. A receptor for protons in the nerve cell membrane. *Neuroscience.* 5:2325–2327.

Kubo, Y., T. J. Baldwin, Y. N. Jan, and L. Y. Jan. 1993. Primary structure and functional expression of a mouse inward rectifier potassium channel. *Nature.* 362:127–133.

Lewis, R. S., and A. J. Hudspeth. 1983. Voltage and ion-dependent conductances in solitary vertebrate hair cells. *Nature.* 304:538–541.

Lopatin, A. N., E. N. Makhina, and C. G. Nichols. 1994. Potassium channel block by cytoplasmic polyamines as the mechanism of intrinsic rectification. *Nature.* 366:366–369.

Matsuda, H. 1988. Open-state substructure of inwardly rectifying potassium channels revealed by magnesium block in guinea-pig heart cells. *J. Physiol. (Lond.).* 397:237–258.

Navaratnam, D. S., L. Escobar, M. Covarrubias, and J. C. Oberholtzer. 1995. Permeation properties and differential expression across the auditory receptor epithelium of an inward rectifier K^+ channel cloned from the chick inner ear. *J. Biol. Chem.* 270:19238–19245.

Neher, E., and H. D. Lux. 1973. Rapid changes of potassium concentration at the outer surface of exposed single neurons during membrane current flow. *J. Gen. Physiol.* 61:385–399.

Nichols, C. G., K. Ho, and S. Hebert. 1994. Mg^{2+}-dependent inward rectification of ROMK1 potassium channels expressed in *Xenopus* oocytes. *J. Physiol. (Lond.).* 476.1:399–409.

Ohmori, H. 1978. Inactivation kinetics and steady-state current noise in the anomalous rectifier of tunicate egg cell membranes. *J. Physiol. (Lond.).* 281:77–99.

Ohmori, H. 1984. Studies of ionic currents in the isolated vestibular hair cell of the chick. *J. Physiol. (Lond.).* 350:561–581.

Pennington, N. J., J. S. Kelly, and A. P. Fox. 1993. Whole-cell recordings of inwardly rectifying K^+ currents activated by 5-HT1A receptors on dorsal raphe neurones of the adult rat. *J. Physiol. (Lond.).* 469:387–405.

Press, W. H., S. A. Teukolsky, W. T. Vetterline, and B. P. Flannery. 1994. Numerical Recipes in C. Cambridge University Press, Cambridge, England.

Sakmann, B., and G. Trube. 1984. Voltage-dependent inactivation of inward-rectifying single-channel currents in the guinea-pig heart cell membrane. *J. Physiol. (Lond.).* 347:659–83.

Salzer, S. J., D. E. Mattox, and W. E. Brownell. 1990. Cochlear damage and increased threshold in alpha-difluoromethylornithine (DFMO) treated guinea pigs. *Hear. Res.* 46:101–112.

Sanguinetti, M. C., and R. S. Kass. 1984. Photoalteration of calcium channel blockade in the cardiac purkinje fiber. *Biophys. J.* 45:873–880.

Schweitzer, L., J. H. Casseday, A. Sjoerdsma, P. P. McCann, and J. V. Bartolome. 1986. Identification of polyamines in the cochlea of the rat and their potential role in hearing. *Brain Res. Bull.* 16:215–218.

Standen, N. B., and P. R. Stanfield. 1979. Potassium depletion and sodium block of potassium currents under hyperpolarization in frog sartorius muscle. *J. Physiol. (Lond.).* 294:497–520.

Stanfield, P. R., N. W. Davies, P. A. Shelton, I. A. Khan, W. J. Brammar, N. B. Standen, and E. C. Conley. 1994a. The intrinsic gating of inward rectifier K^+ channels expressed from the murine IRK1 gene depends on voltage, K^+ and Mg^{2+}. *J. Physiol. (Lond.).* 475.1:1–7.

Stanfield, P. R., N. W. Davies, P. A. Shelton, M. J. Sutcliffe, I. A. Khan, W. J. Brammar, and E. C. Conley. 1994b. A single aspartate residue is involved in both intrinsic gating and blockage by Mg of the inward rectifier, IRK1. *J. Physiol. (Lond.).* 478.1:1–6.

Vandenberg, C. A. 1987. Inward rectification of a potassium channel in cardiac ventricle cells depends on internal magnesium ions. *Proc. Natl. Acad. Sci. USA.* 391:2560–2564.

Wersäll, J. 1956. Studies on the structure and innervation of the sensory epithelium of the cristae ampullares in the guinea pig. *Acta Otolaryngol. Suppl. (Stockh.).* 126:7–85.

Woodhull, A. M. 1973. Ionic blockage of sodium channels in nerve. *J. Gen. Physiol.* 61:687–708.

Wu, Y.-C., J. J. Art, M. B. Goodman, and R. Fettiplace. 1995. A kinetic description of the calcium-activated potassium channel and its application to electrical tuning of hair cells. *Prog. Biophys. Mol. Biol.* 63: 131–158.

Yamaguchi, K., Y. Nakajima, S. Nakajima, and P. R. Stanfield. 1990. Modulation of inwardly rectifying channels by substance P in cholinergic neurones from rat brain in culture. *J. Physiol. (Lond.).* 426: 499–520.